Chapter 4
Function and Acoustics of the Normal and Diseased Middle Ear

Susan E. Voss, Hideko Heidi Nakajima, Alexander M. Huber, and Christopher A. Shera

Keywords Aerated middle ear • Incus motion • Malleus motion • Middle ear cavity • Middle ear disease • Middle ear fluid • Middle ear impedance • Middle ear model • Middle ear pathologies • Middle ear reflectance • Middle ear transfer functions • Ossicular disarticulation • Ossicular fixation • Ossicular motion • Otitis media • Stapes motion • Tympanic-membrane atelectasis • Tympanic-membrane function • Tympanic-membrane perforations • Tympanic-membrane structure • Tympanosclerosis • Tympanostomy tubes

S.E. Voss (✉)
Picker Engineering Program, Smith College, 100 Green St. Ford Hall, Northampton, MA 01063, USA
e-mail: svoss@smith.edu

H.H. Nakajima
Department of Otology and Laryngology, Harvard Medical School, Massachusetts Eye and Ear Infirmary, 243 Charles Street, Boston, MA 02114, USA

Eaton-Peabody Laboratories, Massachusetts Eye and Ear Infirmary, 243 Charles Street, Boston, MA 02114, USA
e-mail: Heidi_Nakajima@meei.harvard.edu

A.M. Huber
Department of Otorhinolaryngology, University Hospital of Zurich, Frauenklinikstrasse 24, 8091 Zurich, Switzerland
e-mail: alex.huber@usz.ch

C.A. Shera
Eaton-Peabody Laboratories, Massachusetts Eye and Ear Infirmary, 243 Charles Street, Boston, MA 02114, USA

S. Puria et al. (eds.), *The Middle Ear: Science, Otosurgery, and Technology*, Springer Handbook of Auditory Research 46, DOI 10.1007/978-1-4614-6591-1_4,

4.1 Introduction

Reviews such as this one usually begin by stating that the primary function of the middle ear is to transfer sound from the air in the ear canal to the fluid in the cochlea. Although the middle ear and its cochlear load do act as an acoustic transformer to provide pressure gain, the system is far better thought of as a wave *transducer*, a device that converts one type of wave at the input into a completely different type on the output. In the ear canal, sound energy propagates as longitudinal (or compressional) waves; in the cochlea, the functionally important motions—those responsible for stimulating the hair cells—are not sound waves in the fluid but transverse, fluid-membrane waves visible in the vibrations of the cochlear partition. These two different types of waves—compressional sound waves in the ear canal and fluid-membrane (or "surface") waves in the cochlea—have very different properties (e.g., amplitudes, wavelengths, wave speeds, and modes of excitation). When driven by sound in the ear canal, the middle ear and cochlea convert the sound into basilar-membrane traveling waves, and vice versa: When driven in reverse by cochlear traveling waves, the middle ear converts these waves into sound in the ear canal (e.g., otoacoustic emissions). This chapter outlines a framework for how this conversion occurs in normal ears and then discusses how a range of middle ear pathologies affect middle ear function. For simplicity, a lumped-element model for the middle ear is employed, modified as necessary to describe various pathologies, to understand measurements of middle ear function in both the normal and the diseased states. The overall goal is to use measurements and models to determine how structural changes in the middle ear are related to changes in its transmission via air conduction pathways. For information on the effect of middle ear pathologies on bone-conduction transmission, see Stenfelt (Chap. 6).

4.2 The Normal Middle Ear

Figure 4.1 shows a conceptual model of the normal middle ear (Peake et al. 1992; Shera and Zweig 1992). The arrival of a sound pressure wave at the eardrum (P_{TM}) triggers a series of events in the middle ear, which consists of those structures within and facing onto the tympanic cavity. In brief, the eardrum oscillates, driven by the pressure difference between the ear canal and tympanic cavity ($P_{TM} - P_{CAV}$). Motion of the eardrum both changes the pressure in the cavity and moves the ossicular chain. Suspended from ligaments and muscles attached to the walls, the three bones of the ossicular chain span the cavity like an arch and transmit the motion of the eardrum to the oval window, where the vibration of the stapes sets the cochlear fluids into motion and generates a pressure difference across the basilar membrane ($P_{OW} - P_{RW}$). The pressure difference drives a fluid-membrane wave that travels along the cochlear partition. Volume displacements of the stapes footplate are relieved by displacement of the round window. Although coupling

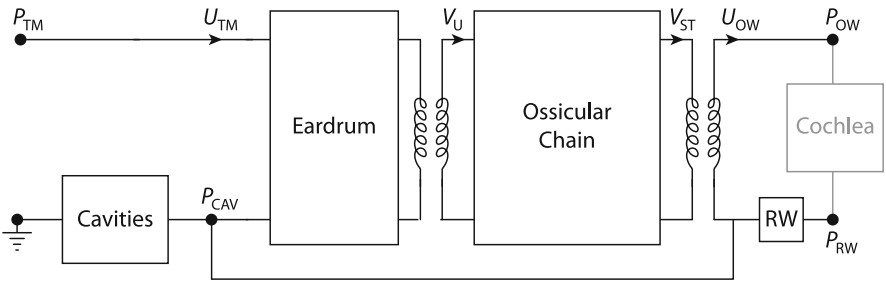

Fig. 4.1 A conceptual model representing the structure and function of the normal middle ear. Components of the middle ear are shown in *black* and the cochlear load is shown in *gray*. When driven in the forward direction, the middle ear converts sound pressure at the tympanic membrane (P_{TM}) into a fluid-membrane wave in the cochlea driven by the intracochlea pressure difference between the oval and round windows ($P_{OW} - P_{RW}$). The eardrum is driven by the pressure difference across its surface, $P_{TM} - P_{CAV}$, where P_{CAV} is the pressure in the tympanic cavity. The cavities, round-window membrane, and cochlear input impedance are represented as one-port impedances (e.g., lumped elements); the eardrum and ossicular chain as more general two-port networks. The transformer inserted between the eardrum and ossicular chain represents the conversion of acoustical to mechanical variables performed by the eardrum (e.g., pressure to force); the transformer between the ossicular chain and cochlea represents the conversion back to acoustic variables performed by the stapes footplate (e.g., velocity to volume velocity). U_{TM} represents the volume velocity of the tympanic membrane and V_U represents the velocity of the umbo, and V_{ST} represents the velocity of the stapes and U_{OW} represents the volume velocity of the oval window (Adapted from Shera and Zweig 1992, and Peake et al. 1992)

to the cochlea through the ossciular chain is stronger, pressure variations in the tympanic cavity also affect the motion of both the stapes and the round window. The middle ear can also be driven "in reverse" by the arrival at the stapes and round window of waves generated or reflected within the cochlea.

4.2.1 Measures of Normal Middle Ear Function

Because the focus of this chapter is the human middle ear, measurements from live and cadaveric human preparations are primarily discussed here. Although live humans provide physiologically ideal preparations, invasive measurements of pressure and motions are limited and often require substantial interpretation. For example, it is not always possible to control parameters such as middle ear pressure or to access measurement locations that would require invasive entry into the middle ear. Measurements on human cadaveric ears have been made to describe middle ear function in normal, diseased, and reconstructed states for more than 100 years (e.g., Helmholtz 1868; von Békésy 1960; Voss et al. 2000). Both Rosowski et al. (1990) and Goode et al. (1993) compared mechanical measurements at the input of the middle ear (acoustic impedance and umbo velocity) made on human cadaveric ears and live ears and showed no statistical differences between the two

groups. More recently, there has been contradictory work regarding whether or not the output of the middle ear (e.g., stapes motion or cochlear pressure) is comparable between live and cadaveric ears, raising question about the possibility of mechanical differences between the two preparations (Huber et al. 2001; Ruggero and Temchin 2003; Chien et al. 2006). However, Chien et al. (2009) showed that the output of the middle ear is comparable for live and cadaveric ears as long as the measurements of the stapes motion are made at the same angle. Thus, when measurements on live human ears are not feasible, it appears that measurements on cadaveric preparations can provide estimates for human middle ear transmission.

The literature includes many examples of middle ear input measures (umbo velocity, impedance, reflectance), middle ear output measures (stapes velocity, intracochlear pressures, audiometry), and combinations of input and output measures that define transfer functions of middle ear output with respect to middle ear input. It is widely recognized that substantial variation exists within a population of normal-hearing ears for any of these measures. Figures 4.2 through 4.4 show representative measurements to demonstrate the general appearance of some of these measures.

Figure 4.2 plots impedance measurements and the corresponding power reflectance from 12 cadaveric ears made within about 3 mm of the tympanic membrane. As numerous reports demonstrate (e.g., Onchi 1961; Zwislocki 1962; Voss et al. 2000), the impedance is compliance dominated at frequencies below about 1,000 Hz, with a magnitude that decreases with increasing frequency at about 20 dB/decade and an angle that is approximately flat with frequency and approaches −0.25 cycles. Above about 1 kHz, the behavior is more complicated, with contributions from both damping and mass-dominated features, and multiple local minima and maxima, with details dependent on the individual ear and likely resulting from both the sound-transmission system of the ear (i.e., tympanic membrane and ossicles) as well as the structure of the middle ear cavities (Stepp and Voss 2005).

The power reflectance is a measure of the amount of sound power reflected from the tympanic membrane. It can be calculated from the impedance and an estimate of the ear-canal cross-sectional area (e.g., Allen 1986; Keefe et al. 1993; Voss et al. 2008). A power reflectance of 1 means that all sound is reflected, and a power reflectance of zero means that all sound is absorbed by the middle ear and cochlea. The example plots here are typical of additional measurements in the literature that show a power reflectance near 1 at the lower, compliance-dominated frequencies; a lower power reflectance near 1–4 kHz where the middle ear absorbs more power; and more variability in power reflectance at the higher frequencies. These middle frequencies (1–4 kHz) where power is most absorbed also correspond to the frequency region where human hearing is known to be most sensitive. Limited measurements of reflectance have been reported at higher frequencies up to 15 kHz (Farmer-Fedor and Rabbitt 2002; Rasetshwane and Neely 2011); the reflectance generally approaches 1 above about 10 kHz, suggesting that the middle ear limits the transmission of pressure waves at these higher frequencies. These higher

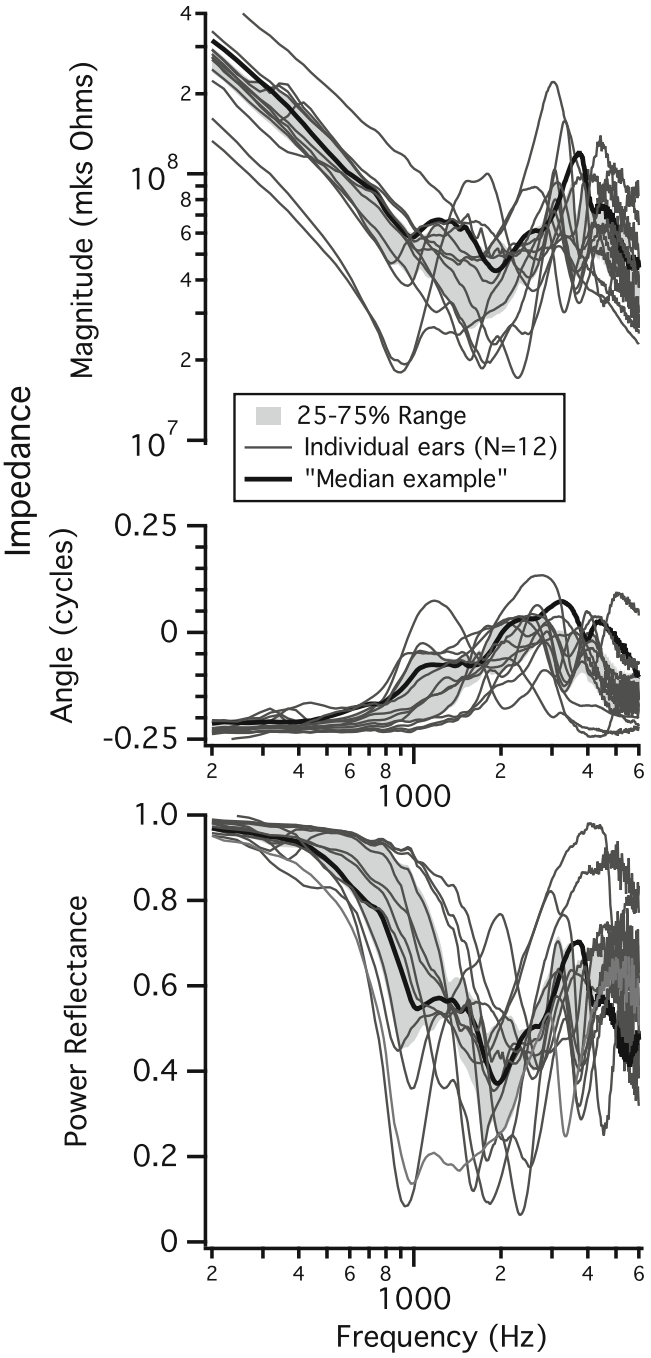

Fig. 4.2 Measurements of impedance magnitudes (*upper row*) and angles (*middle row*) and corresponding calculations of power reflectance (*lower row*) from 12 cadaveric ears described in detail by Voss et al. (2000). Individual ears are plotted with gray lines, the shaded region represents the 25–75% range of all data at each frequency, and the individual ear plotted in black is a representative measurement that approximates the median at most frequencies. The impedance is the ratio between the sound pressure and the volume velocity at the tympanic membrane, and the mks Ohms have fundamental units of N-s/m^5. The power reflectance is calculated from the impedance as $\mathcal{R}(f) = \left|\frac{Z(f)-1}{Z(f)+1}\right|^2$, where $Z(f)$ is the impedance normalized by the ear-canal's characteristic impedance $\rho c/A$, where A is the cross-sectional area of the ear canal, ρ is the density of air, and c is the speed of sound in air

frequency measurements also show substantial variability across subjects; this is an area where more measurements and interpretation are needed.

Figure 4.3 plots the transfer functions of the umbo velocity with respect to the ear-canal sound pressure (left column), the stapes velocity and the ear-canal sound pressure (middle column), and the corresponding stapes-to-umbo-velocity ratio (right column) from a population of cadaveric ears described by Nakajima et al. (2005a). At the lower frequencies, below 0.8–1 kHz, both velocity transfer-function magnitudes increase with frequency at about 20 dB per decade, and both transfer functions have an angle of about 0.25 cycles, consistent with the compliance-dominated impedance measurements described earlier. As frequency increases, the behavior of both velocity transfer functions becomes more complicated; generally the magnitudes exhibit multiple local minima and maxima and the angles decrease with increasing frequency. The stapes-velocity transfer function's angle decreases at a faster rate than the umbo-velocity transfer function's angle, thus leading to an increasing difference in these angles with frequency above about 0.8–1 kHz. The divergence of the stapes and umbo velocity angles here could potentially result from complex three-dimensional motion of the stapes at higher frequencies, as the stapes angle has more variation than that of the umbo. The right column of Fig. 4.3 plots the ratio between the stapes and umbo transfer functions and provides a measure for the velocity gain of the middle ear. At 0.5 kHz, the magnitude gain for the 25–75% of the data range is from 0.17 to 0.36, indicating that the magnitude of stapes velocity is about 9–15 dB smaller than that of the umbo. At higher frequencies there is more variability in this ratio, but the ratio generally decreases further with increasing frequency. The angle difference between the umbo velocity and stapes velocity transfer functions indicates that the stapes and umbo move "in phase" with one another at the lowest frequencies (below about 0.5 kHz), where the angle difference is nearly zero. However, as frequency increases, the angle of the stapes velocity decreases with frequency faster than the angle of the umbo velocity, resulting in a negative angle difference between the two. Thus, at frequencies above 0.5 kHz, the angle of the stapes velocity increasingly lags behind the umbo velocity. In addition, while the vibration mode of the stapes is predominantly piston-like in the low frequencies, its motion becomes increasingly complex with higher frequencies (Sim et al. 2010). Although tilting motions of the stapes do not necessarily lead to bulk movements of cochlear fluids away from the oval window, such vibration modes may also lead to cochlear activity (Huber et al. 2008a). In summary, these measurements of umbo and stapes velocities suggest that the transfer function from the ear canal to the cochlea is both frequency dependent and ear dependent.

Figure 4.4 shows measurements from Puria et al. (1997), Aibara et al. (2001), and Nakajima et al. (2009) of the transfer function between the intracochlear pressure within the scala vestibuli and the ear-canal pressure at the tympanic membrane. This transfer function is largest in the middle frequencies (1–4 kHz), where it approaches a gain of about 20–25 dB. This is the same frequency ranges where the energy reflectance is smallest; thus both measurements are consistent with the largest stimuli reaching the cochlea for 1–4 kHz stimuli.

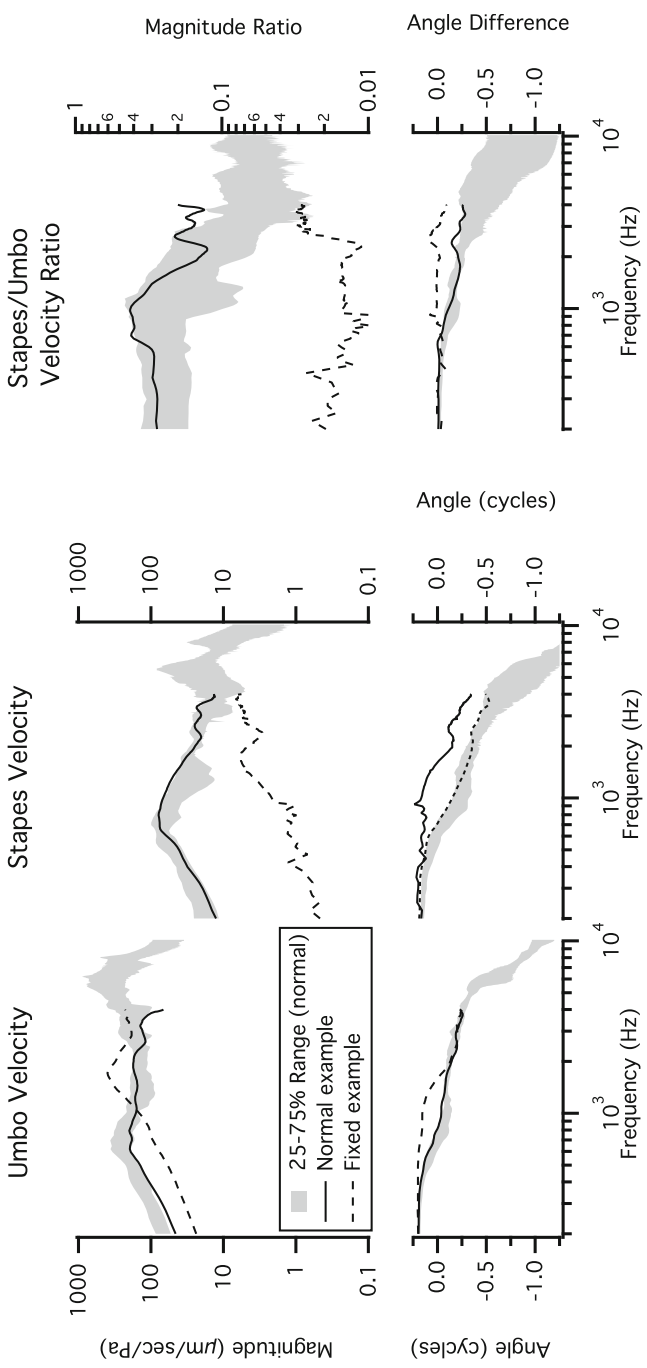

Fig. 4.3 Measurements of umbo velocities (*left column*), stapes velocities (*middle column*), and the ratio stapes-to-umbo-velocity (*right column*). The shaded regions are the 25–75% ranges from 14 normal cadaveric ears described in detail by Nakajima et al. (2005a). One representative individual measurement is plotted with the *solid line* in the normal state and the *dashed line* with the stapes fixed (Discussed later in this chapter)

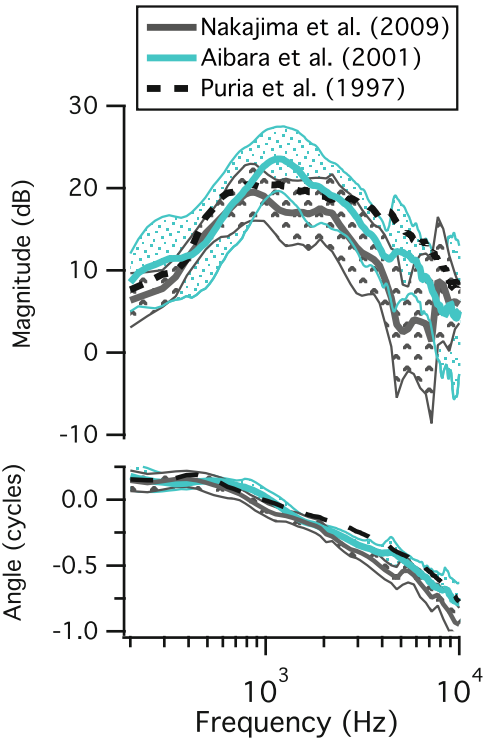

Fig. 4.4 Middle ear pressure gain of scala vestibule pressure to ear-canal pressure from Puria et al. (1997), Aibara et al. (2001), and Nakajima et al. (2009). *Shaded regions* indicate means plus and minus standard deviations

4.2.2 Function of Individual Parts of the Normal Middle Ear

The measurements presented earlier provide a system-level picture for how sound is modified and processed by the middle ear. This section describes the motion of the individual pieces that come together to produce the relatively smooth transfer functions pictured earlier.

4.2.2.1 Tympanic Membrane

It is at the tympanic membrane (TM) where the initial transformation of sound from the ear canal to the cochlea takes place. The unique anatomical shape and material properties of the TM contribute to its motion. Thus the function of the TM relies on the specific motion of the TM and how that motion transduces sound to the middle ear ossicles.

To understand human TM motion, various measurements and studies have been performed. For example, time averaged holograms have been used by Tonndorf and Khanna (1972) and Løkbergand et al. (1979) and more recently by Rosowski et al. (2009).

Speckle holography was used by Wada et al. (2002); scanning laser Doppler vibrometry (LDV) by Konrádsson et al. (1987), Ball et al. (1997), and Decraemer et al. (1999); and stroboscopic holography by Cheng et al. (2010).

Observations of the spatial patterns of TM motion in response to sound suggest an increase in the modes of motion of the surface of the TM with frequency, where the spatial patterns of motion become more complex with higher frequencies, as would be expected of a circular membrane such as a microphone diaphragm (Tonndorf and Khanna 1970; Khanna and Tonndorf 1972). Below 1 kHz, the entire surface of the human and cat TM moves in phase with largest motion in the posterior aspect (Decraemer et al. 1999; Cheng et al. 2010). As frequency increases (2–6 kHz), the motion patterns appear more complicated (Tonndorf and Khanna 1972; Rosowski et al. 2009). At even higher frequencies (8 kHz and above), Rosowski et al. (2009) found that the pattern appears more "ordered," with noticeable circular and radial patterns of motion. Before 2010, many reports of the spatial variations in TM motion depended on time-averaged holography, which is insensitive to the phase of motion, and the complex and ordered motions were hypothesized to represent different modal patterns where in individual modal maxima would move out of phase with surrounding maxima. However, more recent data from high-spatial-density laserdoppler measurements (de La Rochefoucauld and Olson 2010) and stroboscopic holography (Cheng et al. 2010) demonstrate that the phase variations seen along the surface of the TM are more consistent with a traveling wave. de La Rochefoucauld and Olson (2010) noted motion that appeared to be a combination of "wavy" and "piston-like" motion. The stroboscopic holographic data have been interpreted as a combination of both modal motion (standing waves) and traveling waves on the TM surface (Cheng et al. 2010).

Although various studies have measured TM motion, how this motion contributes to the transduction of sound to the cochlea, especially at higher frequencies, is not fully understood. Various theories of how TM motion results in the transduction of sound have been proposed. Helmholtz (1868) proposed that the curved shaped of the TM works as a catenary lever, where large displacements near the annular ring (the outer edge) produce small displacements of the malleus. Later, von Békésy (1941) proposed that the transformation of TM motion to the middle ear was dependent on the area ratio between the TM and stapes footplate and that the curvature of the TM was unimportant. The question of the curvature is still a point of study. The idea that the magnitude of the motion of the manubrium of the malleus is much less than the motion of other areas of the TM has been repeatedly demonstrated with holography (Khanna and Tonndorf 1972; Cheng et al. 2010) and with laser-Doppler measurements (Goode et al. 1996; Decraemer et al. 1999).

Although the modal interpretations of TM motion suggest that those TM regions that move with the manubrium are coupled to it, the presence of traveling waves on the TM surface (Cheng et al. 2010; de La Rochefoucauld and Olson 2010) have led to an alternative theory. If surface waves on the TM actually carry sound energy from the periphery to the center of the TM, it would contribute to a delay in the

middle ear (Olson 1998; Puria and Allen 1998; Parent and Allen 2010). There does seem to be a delay between the sound pressure within the ear canal near the TM and the motion of the stapes or cochlear sound pressure that is characterized by a group delay of 0.04–0.09 ms (O'Connor and Puria 2008; Nakajima et al. 2009). This delay, however, is an order of magnitude faster than the estimated 0.3–1.3 ms for the traveling wave along the human TM measured by the stroboscopic holographic technique (Chen et al. 2012). Similarly, a long traveling-wave delay of 0.18 ms was found on the TM of the gerbil versus a middle ear transmission delay of only 0.025–0.03 ms (de La Rochefoucauld and Olson 2010).

The best described theory of TM traveling waves is that of Puria and Allen (1998), who have proposed that the power of sound in the ear canal is matched to the outer rim of the TM, and that power collected at the rim is conducted to the umbo at the center of the TM via waves that travel on the TM surface. O'Connor and Puria (2008) and Parent and Allen (2007, 2010) further investigated this idea with a transmission line model that matches the impedance between the ear-canal air and TM and between the TM and the ossicles. These idealized models lacked reflections and mode-like standing waves. Measurements show TM surface motions consistent with a combination of two types of motion: de La Rochefoucauld and Olson (2010) described both a wavy and piston-like motion with LDV in the gerbil, and Cheng et al. (2010) described a traveling wave and modal motion with stroboscopic holography in the human. Estimates of the ratio of the magnitude of the two components generally find that the modal component is larger. Because the umbo impedance cannot possibly be matched to the TM impedance perfectly, it is not surprising that both modes are present. There would have to be some reflections at the umbo due to the traveling wave. Whether both, or which one of these components contributes to TM-ossicular sound transduction is still unknown, but is being addressed using computational model techniques.

There is a long history of the use of finite element models to investigate the transduction of sound by the TM (Gan et al. 2002; Koike et al. 2002). Recently, Fay et al. (2006) used a finite-element model to investigate the consequences of the shape of the TM and known material properties and spatial variations in the thickness of the TM; their work suggests that the shape and mechanical variations enable broad impedance matching from the low impedance of the air in the ear canal to the high mechanical impedance at the ossicles. If the eardrum is shaped too deep, high-frequency transmission is lost, while if the eardrum is too shallow, low-frequency transmission is lost. They also predicted that at low frequencies, the eardrum moves in unison, while at higher frequencies, there are many modes of motion. Furthermore, they propose that the close frequency spacing of the natural frequencies of these many modes sum to enable efficient transfer of power with a smooth frequency response. This suggestion is related but different from the observations that TM motion patterns appear dominated by low-order modes of motion. Funnell et al. (1987) also suggested that a spatial integration is likely taking place over the eardrum, allowing for a relatively smooth frequency response in transferring sound.

Additional experiments have been performed to determine how the eardrum's ultrastructure of its radial fibers influences sound transmission. Experiments have demonstrated that for frequencies below 4 kHz, slits in the TM fibers have little effect on the sound transmission, as patching the TM allows the response to return nearly to normal (Voss et al. 2001a; O'Connor et al. 2008). However, O'Connor et al. (2008) also show experiments that are consistent with their conclusion that "Radial collagen fibers in the tympanic membrane play an important role in the conduction of sound above 4 kHz." Thus, understanding the structure–function relationship of the eardrum is an ongoing area of work. Continued detailed experimental measurements in conjunction with realizable models will aid in determining how the TM transduces sound to the ossicles, especially at high frequencies, which is generally unique to mammalian hearing.

4.2.2.2 Malleus and Incus Complex Motion

Two classical hypotheses regarding motion of the malleus–incus complex (MIC) are: (1) the MIC moves as a rigid body without relative motion between the malleus and the incus (Wever and Lawrence 1954; von Békésy 1960) and (2) prevalent motion of the MIC is a hinged rotation about the anterior–posterior axis of the MIC that passes through the center of gravity of the ossicles (Manley and Johnstone 1974). In measurements on cat and human, motions of the MIC are well adapted to the classical hypotheses at low frequencies, and motions of the MIC showed more complicated patterns with change of the rotational axis in all three-dimensional motion components at high frequencies (Decraemer et al. 1991; Decraemer and Khanna 1994; Sim et al. 2004). Relative motions between the malleus and the incus have also been observed (Dahmann 1930; Hüttenbrink 1988; Willi et al. 2002). Puria and Steele (2010) hypothesize that slippage between the malleus and incus evolved as part of several mechanisms that allow for more efficient middle ear function at higher frequencies. A complete description of the actual motion of the MIC and its corresponding importance for sound transmission to the cochlea is an active area of research.

4.2.2.3 Stapes Motion

Though it is often assumed that the stapes moves in a piston-like manner, spatial modes of the stapes vibration have been measured. von Békésy (1960) described rotational motion around an axis near the posterior edge of the footplate, and Kirikae (1960) reported hinged rotation around a posterior axis and rotation around the long axis of the footplate in measurements with a drained cochlea. Recent developments in measurement techniques and methods have shown that motion of the stapes is almost piston-like at low frequencies and contains complex spatial modes at high frequencies (Gyo et al. 1987; Decraemer et al. 2007). In recent studies with human temporal bones, assuming that anatomical features of the stapes annular ring restrict

motions of the stapes footplate in the plane of the footplate, piston-like motion and two rocking-like motions of the stapes (i.e., the two rotational motions along the long and short axes of the footplate) were considered as primary motion components of the human stapes (Hato et al. 2003; Sim et al. 2010). However, it has not been proven that the other components of the stapes motion are insignificant in human middle ear transmission, and Decraemer et al. (2007) reported non-negligible motions through the plane of the footplate in the gerbil stapes.

4.3 The Diseased Middle Ear

4.3.1 Overview

The measurements presented earlier focus on transmission through the normal middle ear. Almost all middle ear models assume that the only mechanism for transmission to the cochlea is from the ossicular chain being driven by the pressure difference across the tympanic membrane and the stapes moving in and out of the oval window; this mode of transmission was termed "ossicular coupling" by Peake et al. (1992). Peake et al. (1992) also emphasize that when the ear is not normal, a mode they term "acoustic coupling" can become important. Acoustic coupling refers to the response of the cochlea to the pressure difference between the pressures adjacent to the oval and round windows, and its contribution is about 60 dB below ossicular coupling when the ear is normal; thus acoustic coupling is important in some specific disease states but has a negligible contribution in the normal ear.

In this section, several middle ear disorders and their effects on middle ear transmission are described. In some cases, the model of Fig. 4.5 can be adapted to fit the disorder, allowing model predictions to be compared to available data. In other cases, no model exists for the specific situation. The specific disorders discussed are grouped into three categories: (1) primarily affecting the middle ear cavity, (2) primarily affecting the tympanic membrane, and (3) primarily affecting the ossicles.

4.3.2 The Middle Ear Cavity

When the ear is normal, the impedance of the middle ear cavity plays a relatively small role in determining transmission through the middle ear; the volume of the cavity is large enough to translate into an impedance that is small compared to the other relevant impedances in the system. In terms of Fig. 4.5, for the normal ear, the combined impedance of the tympanic membrane, ossicular system, and cochlea (often termed Z_{TOC}) has a much larger magnitude than that of the cavity

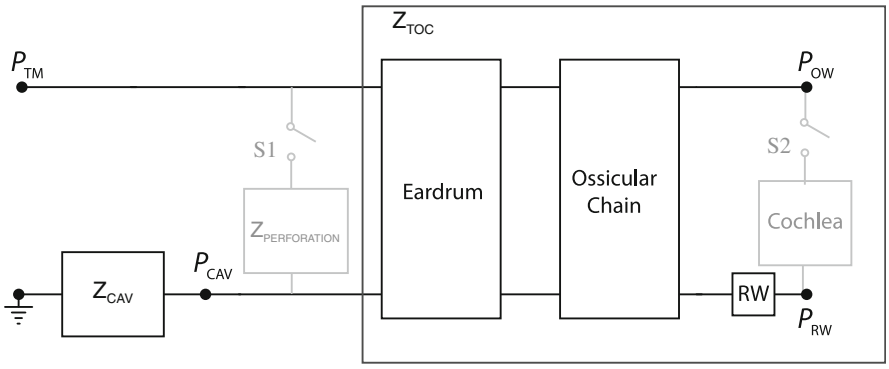

Fig. 4.5 A lumped-element analog model of the middle ear, adapted from Kringlebotn (1988). The two switches, S1 and S2, are included to model the effect of middle ear pathologies. For the normal ear, S1 is open and S2 is closed. With the exception of the middle ear cavities, parameter values are the same as those published by Kringlebotn. For the cavities, two of the values are derived from more recent measurements of Voss et al. (2000) and Stepp and Voss (2005) and are $R_{ad} = 5 \times 10^4 \sqrt{f}$ and $M_{ad} = 1{,}000$. When the middle ear cavity is open to the environment during measurements, the impedance that represents the antrum of the middle ear cavity would be set to 0. When switch S1 is closed to model a perforation, the model values differ from those used by Kringlebotn (1988); see Voss et al. (2001c) for details

Z_{CAV} (e.g., Fig. 2 of Voss et al. 2001c). However, there are several middle ear disorders for which the middle ear cavity becomes important, resulting from the relative magnitudes of the abnormal Z_{TOC} and Z_{CAV}. At its limit, if $|Z_{CAV}| >> |Z_{TOC}|$, then the pressure driving Z_{TOC} approaches zero because $P_{TM} - P_{CAV}$ approaches zero, leading to no movement of the tympanic membrane or ossicular chain. Changes in the relative sizes of $|Z_{CAV}|$ and $|Z_{TOC}|$ can come about by either increases in $|Z_{CAV}|$ or reductions in $|Z_{TOC}|$.

$|Z_{CAV}|$ is increased when the volume of compressible air in the middle ear cavity is reduced. Merchant et al. (1997) refer to the condition of the loss of compressible air within the middle ear cavity as "nonaeration of the middle ear," and point out that this is a common condition within both diseased ears and some postsurgical ears. Diseases such as Eustachian-tube dysfunction can lead to fluid within the middle ear cavity, which reduces the volume of air by exchanging compressible air for incompressible fluid. Rosowski and Merchant (1995) calculated that the middle ear cavity volume should be at least 0.5 cm^3 in order for the ossicular system to be within 10 dB of normal transmission.

$|Z_{TOC}|$ can be reduced in several ways, including TM perforations, TM atelectasis, and interruption of the ossicular chain. These disorders are discussed in subsequent sections, and the middle ear cavity can play an important role in describing transmission within their presence.

The description of middle ear transmission in the presence of middle ear fluid is complicated because the fluid has at least two fundamental effects: (1) reduction of the middle ear cavity volume and (2) mass loading on the TM, ossicles, and windows of the cochlea. Perhaps the most thorough study of transmission through

the fluid-filled ear is by Ravicz et al. (2004); they used measurements on a cadaveric preparation of the ear to draw several important conclusions related to middle ear function with fluid, including: (1) the effects of the viscosity of the fluid are either nonexistent or so small that they were not measurable; (2) for low frequencies (less than 0.8 kHz), changes in umbo velocity result from a decrease in the volume of the middle ear air space and not from mechanical loading of the tympanic membrane; and (3) for higher frequencies (at and above 2 kHz), the primary mechanism for reduction in umbo velocity with fluid is the loading of the tympanic membrane and not the volume of air in the cavity. Gan et al. (2006) also measured the effects of middle ear fluid on umbo velocity in a cadaveric preparation; they demonstrated that for cavities filled at about 50% the umbo motion is reduced primarily at frequencies above about 1 kHz, and as the cavity becomes nearly fully filled the umbo displacement is reduced across all frequencies. These results are consistent with the interpretation that the reduction in air volume will affect the lower frequencies once the air volume is reduced enough. Voss et al. (2012) measured the effects of middle ear fluid on the power reflectance measured in the ear canals of cadavers; as in the umbo velocity measurements, large variations occurred that depended on both the fluid level and the volume of the middle ear cavities. Collectively, this work shows that middle ear transmission can be substantially reduced by middle ear fluid, but there is not a simple description or model for how the change in volume and the loading of fluid on the ossicles affects middle ear function. At its limit of the cavity being completely filled with fluid, the model of Fig. 4.5 would predict no transmission to the cochlea because it would be impossible to move the tympanic membrane and ossicular system within the incompressible middle ear space (i.e., $P_{TM} = P_{CAV}$ because $|Z_{CAV}| >> |Z_{TOC}|$). Indeed, moving forward, finite-element models such as those proposed by Gan and Wang (2007) will likely be helpful in further understanding middle ear function with fluid.

4.3.3 Disorders that Involve the Tympanic Membrane

The tympanic membrane (TM) can be affected by a number of factors, including perforations, the insertion of tympanostomy tubes, scarring, and TM atelectasis. Most of these disorders result from chronic middle ear disease, but perforations can also result from trauma.

4.3.3.1 TM Perforations and Tympanostomy Tubes

Extensive measurements and corresponding models of transmission with TM perforations have been reported (Voss et al. 2001b, c; Mehta et al. 2006). The Voss et al. (2001c) model for the ear with a tympanic-membrane perforation is equivalent to that shown in Fig. 4.5 with switches S1 and S2 closed. This model has a

topology based on the Kringlebotn (1988) model but with an additional component to represent a TM perforation; a similar model for the effect of a tympanostomy tube would share the same topology. Briefly, the impedance of the perforation $Z_{PERFORATION}$, which depends on the thickness of the tympanic membrane and the diameter of the perforation, acts as a shunt for volume velocity to flow directly from the ear canal to the middle ear cavity. Similarly, the impedance for a tympanostomy tube would depend on the tube's length and diameter. Voss et al. (2001b, c) demonstrated that the major mechanism for changes in transmission with most perforations (except very large ones) is the loss of pressure difference across the tympanic membrane that occurs as volume velocity travels through the perforation and not through the ossicular chain. The physical reduction in the tympanic membrane area or other mechanical changes to the membrane have little effect on the transmission changes, thus leaving the eardrum portion of this model intact.

Figure 4.6 shows several types of measurements made on an example cadaveric ear with perforations introduced. All measurements behave in a systematic manner as the perforation size increases. The impedance remains compliant dominated at lower frequencies but with a reduced magnitude. At the lower frequencies the hole in the TM introduces a shunt path for volume velocity to flow directly into the middle ear cavity, and it is the compliant middle ear cavity that dominates the impedance. As frequency increases above about 0.5–1 kHz, the perforation forms a resonance between the mass of air within the perforation and the air volume of the middle ear cavities (analogous to a Helmholz resonator), and at frequencies above the resonant frequency, the ear's response approaches its normal value. The low-frequency power reflectance is substantially reduced from normal with perforations; this reduction does not mean the cochlea is absorbing more energy but instead that the middle ear cavity is absorbing the energy (Voss et al. 2012). Measurements of the stapes velocity show a systematic low-frequency reduction in magnitude with perforations for the lower frequencies, a slight increase in magnitude at the resonant frequency, and they hover around their normal value at higher frequencies. In summary, the measurements and model are consistent in predicting the following general behavior with TM perforations:

1. Loss is largest at the lowest frequency and decreases with increasing frequency.
2. Loss increases as perforation size increases.
3. Loss does not depend on perforation location [an assumption of this model proven experimentally by Voss et al. (2001a)], disproving what had traditionally been assumed within the clinical literature (e.g., Glasscock and Shambaugh 1990; Schuknecht 1993).
4. The dominant loss mechanism is a reduction in the pressure difference across the tympanic membrane.

Voss et al. (2001c) derived an equation to estimate hearing loss under certain conditions as

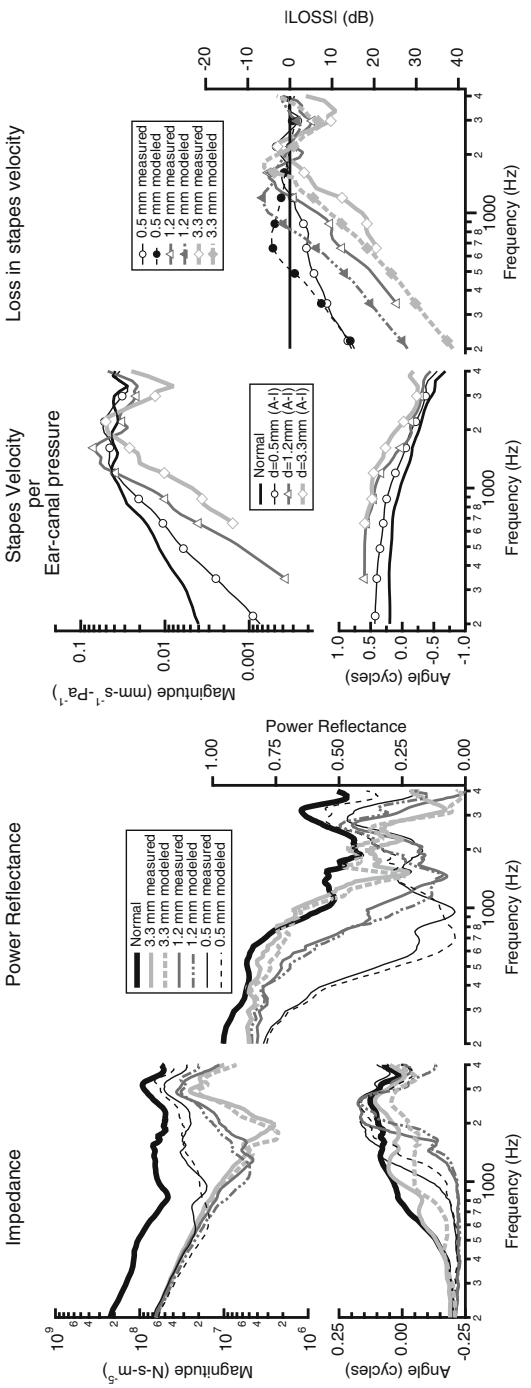

Fig. 4.6 Measurements and model results for an ear with three different sized perforations introduced. (*Left*) Impedance and power reflectance measurements and their corresponding model calculations. (*Right*) Measurements of the stapes velocity per ear-canal sound pressure and measurements and models of the corresponding losses in stapes velocity for each perforation

$$\mathrm{LOSS} = 20\log\left(\left|1 - \frac{\kappa d}{f^2 V}\right|\right), \tag{4.1}$$

where perforation diameter (d) is in millimeters and $d > 1$, frequency (f) is in Hertz and $f < 500$ Hz, middle ear cavity volume V is in cubic centimeters, LOSS is in decibels, and the constant κ equals 2.9×10^6 cm^3 mm^{-1} s^{-2}.

4.3.3.2 TM Atelectasis

TM atelectasis refers to a condition in which the tympanic membrane is displaced medially (retracted). The atelectasis may be of varying severity. It is often the sequella of Eustachian-tube dysfunction producing negative pressure in the middle ear cavity. TM atelactasis can include physical changes to the TM that can affect its coupling to the middle ear system, resulting in a wide range of hearing loss. Merchant et al. (1997) report that hearing loss with atelectasis can range from 0 to 50 dB. Severe TM atelectasis can result in retraction pockets that can be associated with chronic otitis media, cholesteatoma formation, and erosion of the ossicles.

4.3.3.3 Tympanosclerosis

Tympanosclerosis is the formation of white plaques due to hyaline deposits. Such deposits may occur within the TM or in other parts of the middle ear. Tympanosclerosis limited to the TM (also called myringosclerosis) often occurs after chronic inflammation or traumatic events such as TM perforation due to tympanostomy tube placement. This plaque formation can result in a thicker, stiffer eardrum resulting in an abnormal tympanogram. However, tympanosclerosis of the TM may not necessarily affect hearing. Rosowski et al. (2012) showed several examples of abnormal reflectance and umbo-velocity measurements from ears with tympanosclerosis of the TM, although these ears have normal audiograms. Similarly, experimental application of cartilage on the TM produced significant changes in TM motion measured by holography (especially > 4 kHz), but surprisingly did not produce significant changes in transduction of sound measured by stapes motion for the measured frequencies between 0.5 and 8 kHz (Aarnisalo et al. 2009, 2010).

4.3.4 Disorders that Involve the Ossicles

A range of disease processes can affect the ossicles. Disarticulation of the ossicular chain (partial or complete) can be caused by various entities: congenital deformity, as sequelae of chronic otitis media (with or without cholesteatoma), and traumatic

injuries. Ossicular discontinuity commonly occurs at the level of the distal incus near the incudo–stapedial joint, but may also affect other parts of the ossicular chain. Fixation of one or more of the ossicles can result from disease processes such as otosclerosis, as sequelae of chronic otitis media, and from congenital abnormalities. Otosclerosis is a disorder affecting remodeling of the human otic capsule of the temporal bone. Etiology yet remains to be fully explained; however genetic, viral, inflammatory, autoimmune, environmental, and hormonal factors have been implicated (Karosi and Sziklai 2010). Most commonly, the stapes footplate becomes immobilized by otosclerotic bone growth, subsequently reducing sound transmission.

4.3.4.1 Ossicular Disarticulation

Complete ossicular disarticulation, in the presence of an intact tympanic membrane, leads to a reduction of middle ear transmission on the order of 40–60 dB depending on frequency (Merchant et al. 1997; Nakajima et al. 2012). Peake et al. (1992) showed that such a loss in ossicular coupling is consistent with the cochlea responding only to the pressure difference at its oval and round windows (i.e., acoustic coupling). In cadaveric preparations, complete ossicular discontinuity produced reduction in the differential pressure across the partition at the cochlear base (the input signal to the cochlea) similar to clinical audiologic findings, as shown in Fig. 8 of Nakajima et al. (2009). Partial ossicular disarticulation, where there is an insecure connection, often consisting of fibrous tissue, generally results in less conductive hearing loss at low frequencies as compared to high frequencies (Nakajima et al. 2012).

The model in Fig. 4.5 represents the case of incudo–stapedial joint disarticulation when switches S1 and S2 are both open (Voss et al. 2012). Specifically, incus–stapes disarticulation is modeled by connecting the malleus and incus directly to the middle ear air space and bypassing the connection to the cochlea and windows. [In this case, the stapes superstructure remains attached to the cochlea and so the box labeled ossicular chain represents only the malleus and incus; it is assumed that the lack of the relatively small stapes mass here has a negligible effect on the two-port representation of the ossicular chain.] Figure 4.7 shows model predictions and measurements for this disarticulated case. The model predictions for the impedance have a lower magnitude than the normal ear and a lower power reflectance (left column); this behavior results because the malleus and incus are no longer connected to the cochlea but are instead hanging in the middle ear cavity. The low-frequency reduction in power reflectance might naively suggest that sound is absorbed and not reflected, but the sound is actually dissipated within the middle ear cavity and not transferred to the cochlea. Measurements of power reflectance are consistent with the model prediction (right column of Fig. 4.7).

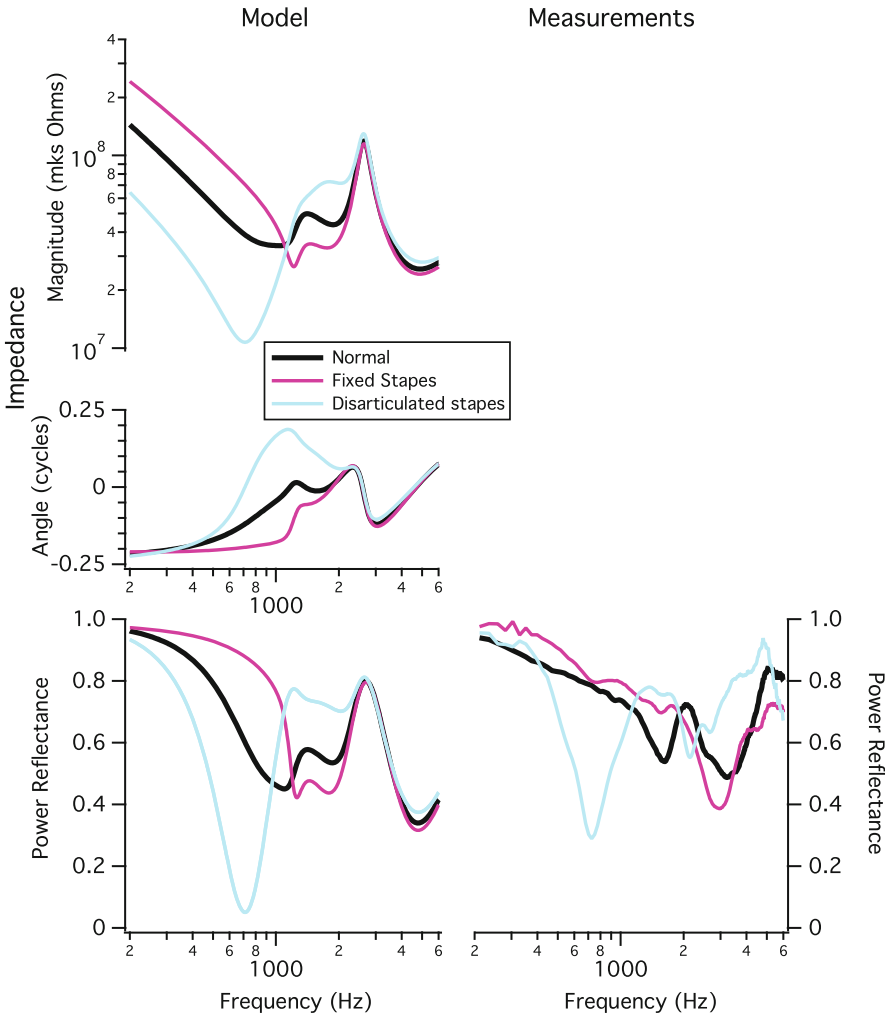

Fig. 4.7 Impedance magnitudes and angles and power reflectance calculations from the models of the ears with the disarticulated incudo–stapedial joint and fixated stapes (*left column*) and corresponding measurements of power reflectance from a cadaveric ear (*right column*) (Voss et al. 2012). Note, measurements are not included for impedances because the measurement was not taken at the TM

4.3.4.2 Fixation of the Ossicles

Stapes fixation most commonly occurs at the level of the footplate and can be caused by otosclerosis or as a result of deposition of fibrous tissue or new bone in cases of chronic otitis media. It is often progressive and can result in conductive hearing loss up to 60 dB, depending on the extent of fixation (Cherukupally et al. 1998). It has been suggested that Ludwig von Beethoven suffered from otosclerosis (Shearer 1990), but unfortunately for him it was not until 1956 that Shea developed

modern stapedectomy surgery with replacement prostheses. Stapedectomy results in surgical reconstruction of the ossicular chain in otosclerosis that offers excellent results with correction of the transmission loss in the vast majority (Huber et al. 2012). In stapedectomy (more accurately stapedotomy), a piston prosthesis drives the oval window through an opening made in the stapes footplate. One end of the prosthesis is attached to the long process of the incus, while the other end of the prosthesis acts as a piston driving through the hole in the footplate, allowing for the piston to produce volume displacement of the cochlear fluid. The properties of this prosthesis play a major role in the functional outcome, with the most important factors being the prosthesis diameter (Rosowski and Merchant 1995; Laske et al. 2011) and fixation characteristics to the incus (Huber et al. 2008b).

Fixation of the malleus head can be caused by formation of fibrous tissue or new bone due to chronic otitis media or as a result of a congenital anomaly. Such malleus head fixation can result in a conductive hearing loss of up to 60 dB (Harris et al. 2002). The malleus can also be "fixed" by increased stiffness of the anterior malleal ligament (which connects the neck of the malleus near the short process anteriorly to the bony wall). It was reported that stiffening of the anterior malleal ligament by hyalinization or calcification results in decreased transduction of sound to the cochlea (Fisch et al. 2001; Huber et al. 2003). However, it was subsequently shown in cadaveric preparations that artificially stiffening the anterior malleal ligament resulted in only insignificant decrease (about 5 dB) of stapes velocity (Nakajima et al. 2005b; Dai et al. 2007). This suggests that such stiffening is not a major source of hearing loss. Because the anterior malleal ligament is along the ossicular axis of rotation for low-frequency stimuli, the stiffening torque at the axis itself would be expected to be small, and this torque is proportional to the distance between the stiffening element and the axis of rotation.

Voss et al. (2012) modified the model of Fig. 4.5 (with S1 open and S2 closed) to represent the case of stapes fixation by increasing the impedance of the annular ligament through a decrease in the compliance of the annular ligament (C_c); as this impedance goes toward infinity, the volume velocity within the circuit that represents stapes motion goes toward zero. Because fixation occurs in varying degrees, Voss et al. (2012) altered this compliance C_c instead of simply making it an open circuit, and here it is reduced by a factor of 0.01. Figure 4.7 shows that model predictions for the fixed stapes case have a higher impedance magnitude and higher power reflectance than a normal ear at the lower frequencies (left column). Voss et al. (2012) also show that as the model's annular-ligament impedance approaches infinity, the changes from normal in reflectance reach a limit; the interpretation is that there are multiple compliances in the middle ear system that affect the impedance and reflectance so that even when the stapes is effectively immobile there is still movement within the middle ear system. Nakajima et al. (2005a) show that fixation of the stapes does not result in large decreases in umbo velocity due to the significant flexibility in the ossicular joints (Fig. 4.3). One shortcoming of current lumped-element models (Kringlebotn 1988; Voss et al. 2012) is that they do a poor job of predicting the umbo velocity for the fixed stapes manipulation, possibly due to the need for better representation of the compliances between the ossicular joints.

4.4 Summary

This chapter outlines a framework for how sound in the ear canal is converted from a compressional sound wave to a fluid-membrane wave in the cochlea. In particular, several types of middle ear measures are discussed (e.g., impedance, ossicular vibration, cochlear fluid pressure) and shown to be relatively smooth with frequency. At the same time, complicated and multidimensional motions of the TM and ossicular subsystems have been measured. It remains an active research area to understand how these complicated subsystem motions come together to form the seemingly simple and smooth transfer functions between the cochlea and ear canal. This chapter also employs a lumped-element model to provide a theoretical framework for understanding how some middle ear disorders influence middle ear function for frequencies below about 6 kHz. (e.g., TM perforations, stapes fixation, and stapes disarticulation); the model is less helpful for the conditions of middle ear fluid or cholesteatoma.

Acknowledgments We thank the late Dr. Saumil N. Merchant for many helpful discussions relating to the clinical aspects of the work discussed here. We also thank Mike Ravicz for his extensive help in putting together older data sets for our use in some of the figures. Several colleagues provided substantial help in clarifying the most recent and important aspects of middle ear function: Dr. Jae Hoon helped us to summarize work related to ossicular motion, and Drs. John Rosowski and Lisa Olson helped us to describe recent work on tympanic-membrane motion. We thank Dr. Sunil Puria for his thorough and thoughtful comments that led to great improvements in the overall presentation. This work was supported by the National Institutes of Health (S. E. Voss, H. H. Nakajima, and C. A. Shera) and the National Science Foundation (S. E. Voss).

References

Aarnisalo, A. A., Cheng, J. T., Ravicz, M. E., Hulli, N., Harrington, E. J., Hernandez-Montes, M. S., Furlong, C., Merchant, S. N., & Rosowski, J. J. (2009). Middle ear mechanics of cartilage tympanoplasty evaluated by laser holography and vibrometry. *Otology & Neurotology*, 30, 1209–1214.

Aarnisalo, A. A., Cheng, J. T., Ravicz, M. E., Furlong, C., Merchant, S. N., & Rosowski, J. J. (2010). Motion of the tympanic membrane after cartilage tympanoplasty determined by stroboscopic holography. *Hearing Research*, 263, 78–84.

Aibara, R., Welsh, J. T., Puria, S., & Goode, R. L. (2001). Human middle-ear sound transfer function and cochlear input impedance. *Hearing Research*, 152, 100–109.

Allen, J. B. (1986). Measurement of eardrum acoustic impedance. In J. B. Allen, J. L. Hall, A. Hubbard, S. T. Neely, & A. Tubis (Eds.), *Peripheral auditory mechanisms* (pp. 44–51). New York: Springer-Verlag.

Ball, G. R., Huber, A., & Goode, R. L. (1997). Computerized laser doppler interferometric scanning of the vibrating tympanic membrane. *Ear, Nose, & Throat Journal*, 76, 213–218.

Chen, J. T., Hamade, M., Harrington, E., Furlong, C., Merchant, S. N., & Roswoski, J. J. (2012). Wave motion on the surface of the human membrane: holographic measurement and modeling analysis. *Journal of the Acoustical Society of America*, in press.

Cheng, J. T., Aarnisalo, A. A., Harrington, E., Hernandez-Montes, M. S., Furlong, C., Merchant, S. N., & J. Rosowski, J. (2010). Motion of the surface of the human tympanic membrane measured with stroboscopic holography. *Hearing Research*, 263, 66–77.

Cherukupally, S., Merchant, S., & Rosowski, J. J. (1998). Correlations between pathologic changes in the stapes and conductive hearing loss in otosclerosis. *The Annals of Otology, Rhinology, and Laryngology*, 107, 319–326.

Chien, W., Ravicz, M., Merchant, S., & Rosowski, J. (2006). The effect of methodological differences in the measurement of stapes motion in live and cadaver ears. *Audiology & Neuro-otology*, 11, 183–197.

Chien, W., Rosowski, J. J., Ravicz, M. E., Rauch, S. D., Smullen, J., & Merchant, S. N. (2009). Measurements of stapes velocity in live human ears. *Hearing Research*, 249, 54–61.

Dahmann, H. (1930). Zur physiologie des hörens; experimentelle untersuchungen über die mechanik der gehörknöchelchenkette sowie über deren verhalten auf ton und luftdruck. *Hals–Nasen–Ohrenheilkunde*, 27, 329–368.

Dai, C., Cheng, T., Wood, M. W., & Gan, R. Z. (2007). Fixation and detachment of superior and anterior malleolar ligaments in human middle ear: Experiment and modeling. *Hearing Research*, 230, 24–33.

Decraemer, W. F., Khanna, S. M., & Funnell, W. R. J. (1991). Malleus vibration model changes with frequency. *Hearing Research*, 54, 305–318.

Decraemer, W. F., & Khanna, S. M. (1994). Modelling the malleus vibration as a rigid body motion with one rotational and one translational degree of freedom. *Hearing Research*, 72, 1–18.

Decraemer, W., Khanna, S., & Funnell, W. (1999). Measurement and modeling of the three-dimensional vibration of the stapes in cat. In *Abstracts of the Symposium on Recent Developments in Auditory Mechanics*.

Decraemer, W. F., de La Rochefoucauld, O., Dong, W., Khanna, S. M., & Olson, E. S. (2007). Scala vestibuli pressure and three-dimensional stapes velocity measured in direct succession in gerbil. *Journal of the Acoustical Society of America*, 121, 2774–2791.

de La Rochefoucauld, O., & Olson, E. S. (2010). A sum of simple and complex motions on the eardrum and manubrium in gerbil. *Hearing Research*, 263, 9–15.

Farmer-Fedor, B. L., & Rabbitt, R. D. (2002). Acoustic intensity, impedance and reflection coefficient in the human ear canal. *Journal of the Acoustical Society of America*, 112, 600–620.

Fay, J. P., Puria, S., & Steele, C. R. (2006). The discordant eardrum. *Proceedings of the National Academy of Sciences of the USA*, 103, 19743–19748.

Fisch, U., Acar, G. O., & Huber, A. M. (2001). Malleostapedotomy in revision surgery for otosclerosis. *Otology & Neurotology*, 22, 776–785.

Funnell, W. R., Decraemer, W. F., & Khanna, S. M. (1987). On the damped frequency response of a finite-element model of the cat eardrum. *Journal of the Acoustical Society of America*, 81, 1851–1859.

Gan, R. Z., & Wang, X. (2007). Multifield coupled finite element analysis for sound transmission in otitis media with effusion. *Journal of the Acoustical Society of America*, 122, 3527–3538.

Gan, R. Z., Sun, Q., Dyer, R. K., Jr., Chang, K. H., & Dormer, K. J. (2002). Three-dimensional modeling of middle-ear biomechanics and its applications. *Otology & Neurotology*, 23, 271–280.

Gan, R. Z., Sun, Q., Feng, B., & Wood, M. W. (2006). Acoustic-structural coupled finite element analysis for sound transmission in human ear—Pressure distributions. *Medical Engineering & Physics*, 28, 395–404.

Glasscock, M. E., & Shambaugh, G. E. (1990). *Surgery of the ear*, 4th edition. Philadelphia: W. B. Saunders.

Goode, R. L., Ball, G., & Nishihara, S. (1993). Measurement of umbo vibration in human subjects—method and possible clinical applications. *American Journal of Otology*, 14(3), 247–251.

Goode, R. L., Ball, G., Nishihara, S., & Nakamura, K. (1996). Laser doppler vibrometer (ldv)—a new clinical tool for the otologist. *American Journal of Otology*, 17, 813–822.

Gyo, K., Aritomo, H., & Goode, R. L. (1987). Measurement of the ossicular vibration ratio in human temporal bones by use of a video measuring system. *Acta Oto-Laryngologica*, 103, 87–95.

Harris, J. P., Mehta, R. P., & Nadol, J. B. (2002). Malleus fixation: Clinical and histopathologic findings. *The Annals of Otology, Rhinology, and Laryngology*, 111, 246–254.

Hato, N., Stenfelt, S., & Goode, R. L. (2003). Three-dimensional stapes footplate motion in human temporal bones. *Audiology & Neuro-otology*, 8, 40–152.

Helmholtz, H. L. (1868). Die mechanik der gehörknöchelchen und des trommelfells. *Pflüg Archives European Journal of Physiology*, 1–60.

Huber, A., Linder, T., Ferrazzini, M., Schmid, S., Dillier, N., Stoeckli, S., & Fisch, U. (2001). Intraoperative assessment of stapes movement. *The Annals of Otology, Rhinology, and Laryngology*, 110, 31–35.

Huber, A., Sequeira, D., Breuninger, C., & Eiber, A. (2008a). The effects of complex stapes motion on the response of the cochlea. *Otology & Neurotology*, 29, 1187–1192.

Huber, A., Veraguth, D., Schmid, S., Roth, T., & Eiber, A. (2008b). Tight stapes prosthesis fixation leads to better functional results in otosclerosis surgery. *Otology & Neurotology*, 3292, 893–899.

Huber, A., Schrepfer, T., & Eiber, A. (2012). Clinical evaluation of the NiTi-BOND stapes prosthesis, an optimized shape memory alloy design. *Otology & Neurotology*, 33, 132–136.

Huber, A. M., Koike, T., Wada, H., Nandapalan, V., & Fisch, U. (2003). Fixation of the anterior mallear ligament: Diagnosis and consequences for hearing results in stapes surgery. *The Annals of Otology, Rhinology, and Laryngology*, 112, 348–355.

Hüttenbrink, K. (1988). The mechanics of the middle ear at static air pressures. *Acta Oto-Laryngologica Supplement—*, 451, 1–35.

Karosi, T. & Sziklai, I. (2010). Etiopathogenesis of otosclerosis. *European Archives of Oto-Rhino-Laryngology*, 267, 1337–1349.

Keefe, D. H., Bulen, J. C., Arehart, K. H., & Burns, E. M. (1993). Ear-canal impedance and reflection coefficient in human infants and adults. *Journal of the Acoustical Society of America*, 94(5), 2617–2638.

Khanna, S. M., & Tonndorf, J. (1972). Tympanic membrane vibrations in cats studied by time-averaged holography. *Journal of the Acoustical Society of America*, 51(6), 1904–1920.

Kirikae, I. (1960). *The structure and function of the middle ear*. Tokyo: University of Tokyo Press.

Koike, T., Wada, H., & Kobayashi, T. (2002). Modeling of the human middle ear using the finite-element method. *Journal of the Acoustical Society of America*, 111, 1306–1317.

Konrádsson, K. S., Ivarsson, A., & Bank, G. (1987). Scanning laser doppler vibrometry of the middle ear ossicles. *Scandinavian Audiology*, 16, 159–166.

Kringlebotn, M. (1988). Network model for the human middle ear. *Scandinavian Audiology*, 17, 75–85.

Laske, R., Röösli, C., Chatzimichalis, M., Sim, J., & Huber, A. M. (2011). The influence of prosthesis diameter in stapes surgery: A meta-analysis and systematic review of the literature. *Otology & Neurotology*, 32, 520–528.

Løkbergand, O. J., Høgmoen, K., & Gundersen, T. (1979). On holographic-interferometric investigations of the membrana tympani (living man). In G. v. Bally (Ed.), *Holography in medicine and biology* (11. 212–217). Berlin: Springer-Verlag.

Manley, G. A., & Johnstone, B. M. (1974). Middle-ear function in the guinea pig. *Journal of the Acoustical Society of America*, 56, 571–576.

Mehta, R. P., Rosowski, J. J., Voss, S. E., O'Neil, E., & Merchant, S. N. (2006). Determinants of hearing loss in perforations of the tympanic membrane. *Otology & Neurotology*, 27, 136–143.

Merchant, S. N., Ravicz, M. E., Puria, S., Voss, S. E., Whittemore, K. R., Jr., Peake, W. T., & Rosowski, J. J. (1997). Analysis of middle-ear mechanics and application to diseased and reconstructed ears. *American Journal of Otology*, 18, 139–154.

Nakajima, H. H., Ravicz, M. E., Merchant, S. N., Peake, W. T., & Rosowski, J. J. (2005a). Experimental ossicular fixations and the middle ear's response to sound: Evidence for a flexible ossicular chain. *Hearing Research*, 204, 60–77.

Nakajima, H. H., Ravicz, M. E., Rosowski, J. J., Peake, W. T., & Merchant, S. N. (2005b). Experimental and clinical studies of malleus fixation. *The Laryngoscope*, 115, 147–154.

Nakajima, H. H., Dong, W., Olson, E. S., Merchant, S. N., Ravicz, M. E., & Rosowski, J. J. (2009). Differential intracochlear sound pressure measurements in normal human temporal bones. *Journal of the Association for Research in Otolaryngology*, 10, 23–36.

Nakajima, H. H., Pisano, D. V., Roosli, C., Hamade, M. A., Merchant, G. R., Mafoud, L., Halpin, C. F., Rosowski, J. J., & Merchant, S. N. (2012). Comparison of ear-canal reflectance and umbo velocity in patients with conductive hearing loss: A preliminary study. *Ear and Hearing*, 33, 35–43.

O'Connor, K. N., & Puria, S. (2008). Middle-ear circuit model parameters based on a population of human ears. *Journal of the Acoustical Society of America*, 123(1), 197–211.

O'Connor, K. N., Tam, M., Blevins, N. H., & Puria, S. (2008). Tympanic membrane collagen fibers: A key to high-frequency sound conduction. *The Laryngoscope*, 118, 483490.

Olson, E. S. (1998). Observing middle and inner ear mechanics with novel intracochlear pressure sensors. *Journal of the Acoustical Society of America*, 103, 3445–3463.

Onchi, Y. (1961). Mechanism of the middle ear. *Journal of the Acoustical Society of America*, 33, 794–805.

Parent, P., & Allen, J. B. (2007). Wave model of the cat tympanic membrane. *Journal of the Acoustical Society of America*, 122, 918–931.

Parent, P., & Allen, J. B. (2010). Time-domain wave model of the human tympanic membrane. *Hearing Research*, 263, 152–167.

Peake, W., Rosowski, J. J., & Lynch, T. J. (1992). Middle-ear transmission: Acoustic versus ossicular coupling in cat and human. *Hearing Research*, 57, 245–268.

Puria, S., & Allen, J. B. (1998). Measurements and model of the cat middle ear: Evidence of tympanic membrane acoustic delay. *Journal of the Acoustical Society of America*, 104, 3463–3481.

Puria, S., & Steele, C. (2010). Tympanic membrane and malleus-incus-complex co-adaptations for high-frequency hearing in mammals. *Hearing Research*, 263, 183–190.

Puria, S., Peake, W. T., & Rosowski, J. J. (1997). Sound-pressure measurements in the cochlear vestibule of human-cadaver ears. *Journal of the Acoustical Society of America*, 101, 2754–2770.

Rasetshwane, D. M., & Neely, S. T. (2011). Inverse solution of ear-canal area function from reflectance. *Journal of the Acoustical Society of America*, 130, 3873–3881.

Ravicz, M., Rosowski, J., & Merchant, S. (2004). Mechanisms of hearing loss resulting from middle-ear fluid. *Hearing Research*, 195, 103–130.

Rosowski, J. J., & Merchant, S. N. (1995). Mechanical and acoustic analysis of middle ear reconstruction. *American Journal of Otology*, 16, 486–497.

Rosowski, J. J., Davis, P. J., Merchant, S. N., Donahue, K. M., & Coltrera, M. D. (1990). Cadaver middle ears as models for living ears: Comparisons of middle ear input impedance. *The Annals of Otology, Rhinology, and Laryngology*, 99(5), 403–412.

Rosowski, J. J., Cheng, J. T., Ravicz, M. E., Hulli, N., Harrington, E. J., Mdel, S. H.-M., & Furlong, C. (2009). Computer-assisted time-averaged holography of the motion of the surface of the tympanic membrane with sound stimuli of 0.4 to 25 khz. *Hearing Research*, 253, 83–96.

Rosowski, J. J., Nakajima, H. H., Hamade, M. A., Mafoud, L., Merchant, G. R., Halpin, C. F., & Merchant, S. N. (2012). Ear-canal reflectance, umbo velocity and tympanometry in normal hearing adults. *Ear and Hearing*, 33, 19–34.

Ruggero, M. A., & Temchin, A. N. (2003). Middle-ear transmission in humans: Wide-band, not frequency-tuned? *Acoustic Research Letters Online*, 4, 53–58.

Schuknecht, H. F. (1993). *Pathology of the ear*, 2nd edition. Malvern, PA: Lea & Febiger.

Shearer, P. (1990). The deafness of Beethoven: An audiologic and medical overview. *American Journal of Otology*, 11, 370–374.

Shera, C. A., & Zweig, G. (1992). Middle-ear phenomenology: The view from the three windows. *Journal of the Acoustical Society of America*, 92(3), 1356–1370.

Sim, J., Puria, S., & Steele, C. R. (2004). Three-dimensional measurement and analysis of the isolated malleus-incus complex. In K. Gyo & H. Wada (Eds.), *The 3rd International Symposium on Middle Ear Mechanics in Research and Otology*, (pp. 61–67). Singapore: World Scientific.

Sim, J., Chatzimichalis, M., Lauxmann, M., Rsli, C., Eiber, A., & Huber, A. (2010). Complex stapes motions in human ears. *Journal of the Association for Research in Otolaryngology*, 11, 329–341.

Stepp, C. E., & Voss, S. E. (2005). Acoustics of the human middle-ear air space. *Journal of the Acoustical Society of America*, 118, 861–871.

Tonndorf, J., & Khanna, S. M. (1970). The role of the tympanic membrane in middle ear transmission. *Journal for Oto-Rhino-Laryngology and Its Related Specialties*, 79, 743–753.

Tonndorf, J., & Khanna, S. M. (1972). Tympanic membrane vibrations in human cadaver ears studied by time-averaged holography. *Journal of the Acoustical Society of America*, 52, 1221–1233.

von Békésy, G. (1941). On the measurement of the amplitude of vibration of the ossicles with a capacitive probe [in German]. *Akustische Zeitschrift*, 6.

von Békésy, G. (1960). *Experiments in hearing*. Edited by E. G. Wever. New York: McGraw-Hill.

Voss, S., Horton, N., Woodbury, R., & Sheffield, K. (2008). Sources of variability in reflectance measurements on normal cadaver ears. *Ear and Hearing*, 29, 651–655.

Voss, S., Merchant, G. R., & Horton, N. J. (2012). Effects of middle-ear disorders on power reflectance measured in cadaveric ear canals. *Ear and Hearing*, 33, 195–208.

Voss, S. E., Rosowski, J. J., Merchant, S. N., & Peake, W. T. (2000). Acoustic responses of the human middle ear. *Hearing Research*, 150, 43–69.

Voss, S. E., Rosowski, J. J., Merchant, S. N., & Peake, W. T. (2001a). How do tympanic-membrane perforations affect human middle-ear sound transmission? *Acta Oto-Laryngologica*, 121, 169–173.

Voss, S. E., Rosowski, J. J., Merchant, S. N., & Peake, W. T. (2001b). Middle-ear function with tympanic-membrane perforations. I. Measurements and mechanisms. *Journal of the Acoustical Society of America*, 110, 1432–1444.

Voss, S. E., Rosowski, J. J., Merchant, S. N., & Peake, W. T. (2001c). Middle-ear function with tympanic-membrane perforations. II. A simple model. *Journal of the Acoustical Society of America*, 110, 1445–1452.

Wada, H., Ando, M., Takeuchi, M., Sugawara, H., & Koike, T. (2002). Vibration measurement of the tympanic membrane of guinea pig temporal bones using time averaged speckle pattern interferometry. *Journal of the Acoustical Society of America*, 111, 2189 2199.

Wever, E. G., & Lawrence, M. (1954). *Physiological acoustics*. Princeton, NJ: Princeton University Press.

Willi, U. B., Ferranzzini, M. A., & Huber, A. M. (2002). The incudo-malleolar joint and sound transmission losses. *Hearing Research*, 174, 32–44.

Zwislocki, J. (1962). Analysis of the middle-ear function. Part 1: Input impedance. *Journal of the Acoustical Society of America*, 34, 1514–1523.